Electronic Supplementary Information

Polyethersulfones upcycling to luminescent materials by aminolysis

Johan Liotier[a], Leila Issoufou Alfari[b], Benoit Mahler[b], Thomas Niehaus[b], Christophe Dujardin[b], Simon Guelen[c], Vincent Schanen[c], Véronique Dufaud[a*], Jean Raynaud[a*] and Vincent Monteil[a*]

Table of Contents

1. General procedure for aminolysis of PES

Amine (2-3 eq) and NaH (60 % in mineral oil, 2-3 eq) were placed under argon atmosphere. DMF (30 mL) was then added to solubilise the starting materials. The reaction mixture was stirred at room temperature for 20 minutes. **PES** (500 mg, 2.15 mmol of repeating units, 1 eq) was then added as a solid to the reaction mixture. **PES** solubilized quickly in the solution and the reaction mixture was then heated to the desired temperature for 24 h. After reaction, the mixture was poured into iced water and acidified with 2M HCl. Upon this treatment, the solid products were filtered off whereas the filtrate was extracted 3 times with EtOAc. The organic phases were dried over Na_2SO_4, filtered and the solvent was evaporated to yield pure **BPS**. On the other hand, the solid product was purified by silica gel column chromatography. The elution of the column was carried out gradually. First, a mixture of heptane/EtOAc: 90/10 was used as eluent to remove the excess of aryl amine. Then, a mixture of heptane/EtOAc: 80/20 was used to obtain the di-aminated product, followed by a mixture of heptane/EtOAc: 60/40 to obtain the mono-aminated product. Finally, a mixture of EtOAc/EtOH: 90/10 was used to recover the remaining dimer.

Table 1, Entry 1:

tBuDPA (1.21 g, 4.3 mmol, 2 eq) and NaH (60 % in mineral oil, 157 mg, 4.3 mmol, 2 eq) were reacted at 100 °C. No small molecules were obtained in these conditions, only oligomer products, therefore no purification by chromatographic column was performed.

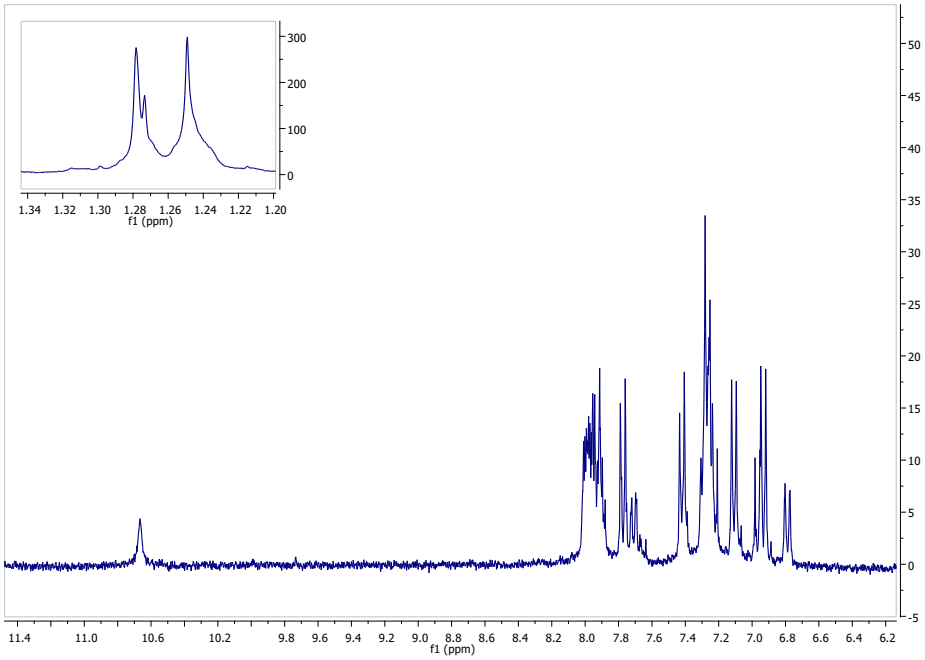

Figure S1: ^{1}H NMR of the solid product of entry 1 (DMSO-d_6, 300 MHz).

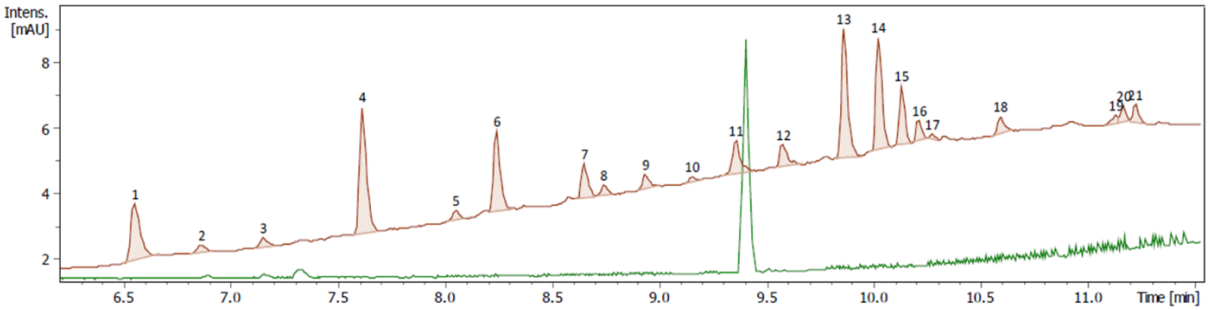

Figure S2: LC chromatogram of the solid product of entry 1.

Table 1, Entry 2:

tBuDPA (1.21 g, 4.3 mmol, 2 eq) and NaH (60 % in mineral oil, 157 mg, 4.3 mmol, 2 eq) were reacted at 120 °C. Some **BPS** (92.4 mg, 731 µmol, 34 %) was obtained but the filtered product was not purified due to the remaining presence of oligomers.

BPS:

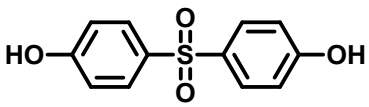

^{1}H NMR (300 MHz, DMSO-d_6) δ 10.52 (s, 2H), 7.70 (d, J = 8.3 Hz, 4H), 6.90 (d, J = 8.3 Hz, 4H).
^{13}C NMR (75 MHz, DMSO-d_6) δ 161.56, 132.03, 129.30, 115.91.
HRMS (ESI-TOF): calculated for $C_{12}H_{10}O_4S$: 251.0373, found: 251.0375.

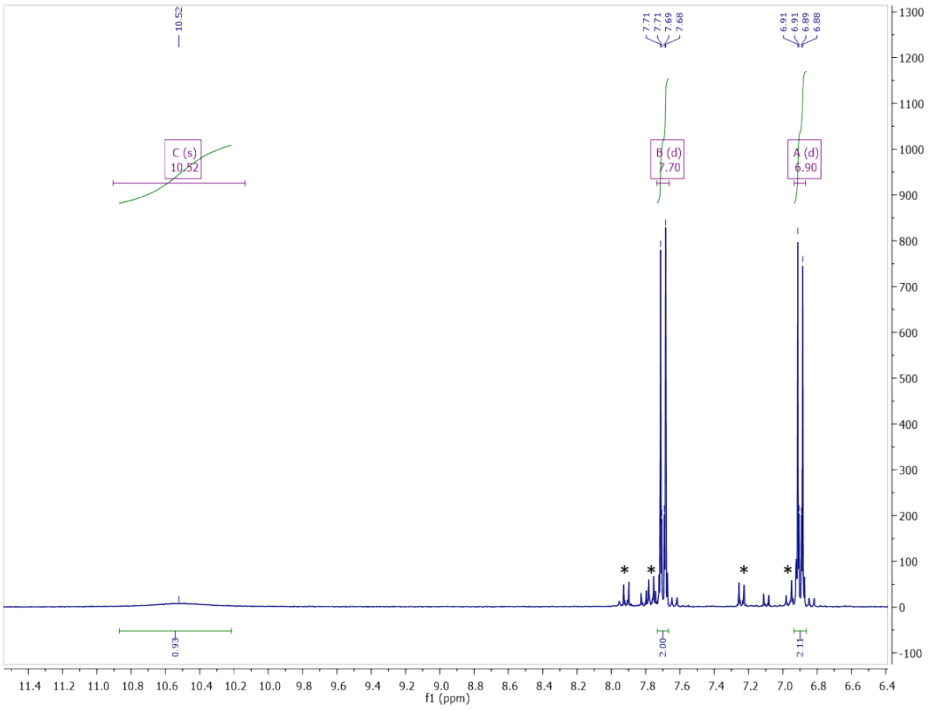

Figure S3 : ^{1}H NMR of **BPS** obtained in entry 2 (DMSO-d_6, 300 MHz). *Signals corresponding to the dimer that displays partially solubility in water and thus has been extracted in a limited amount with the BPS monomer (see also Figure S9).

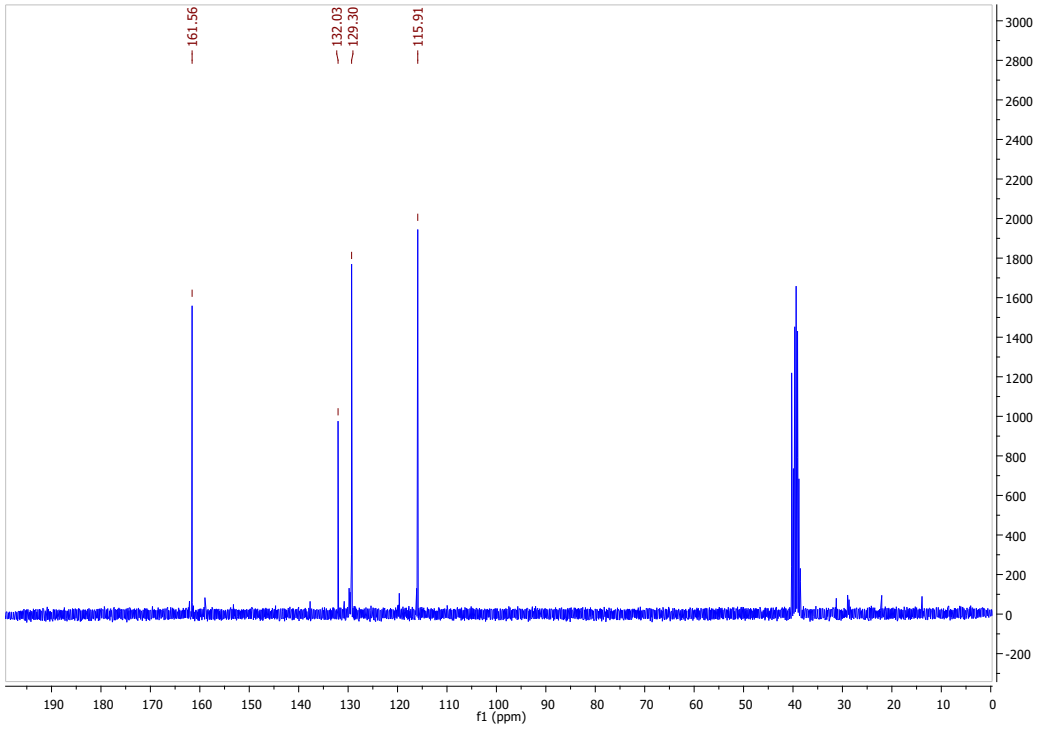

Figure S4: ^{13}C NMR of **BPS** obtained in entry 2 (DMSO-d_6, 75 MHz).

Solid product:

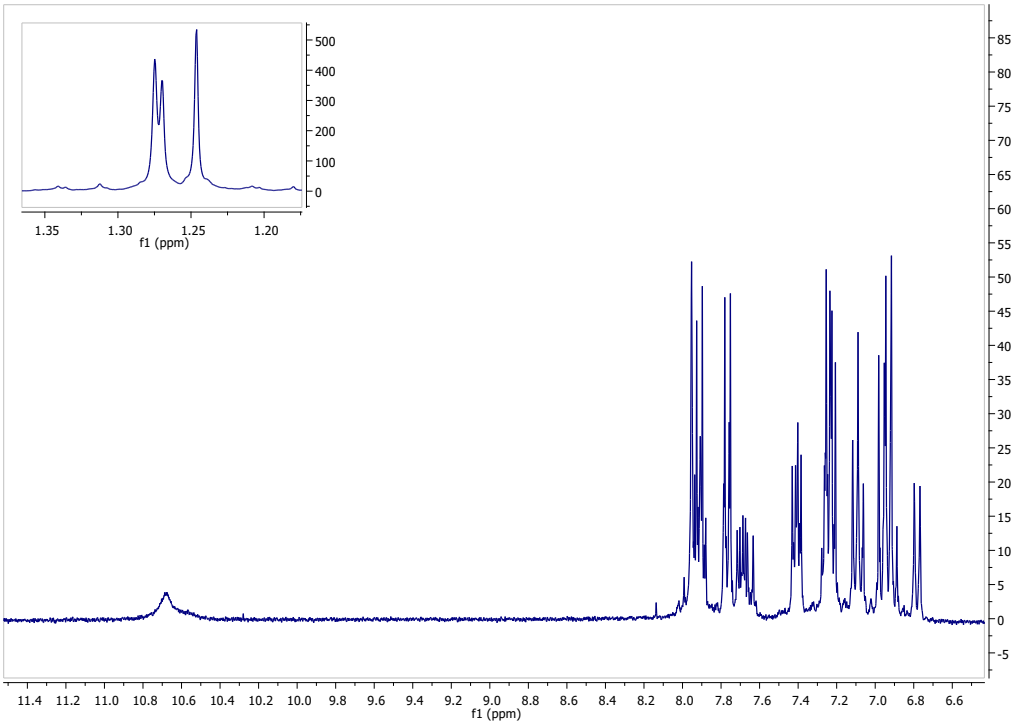

Figure S5: ^{1}H NMR of the solid product of entry 2 (DMSO-d_6, 300 MHz).

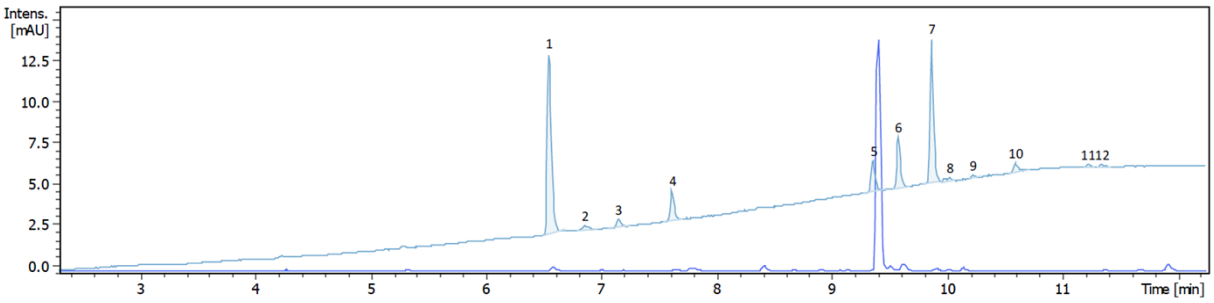

Figure S6: LC chromatogram of the solid product of entry 2.

Table 1, Entry 3:

tBuDPA (1.82 g, 6.45 mmol, 3 eq) and NaH (60 % in mineral oil, 257.98 mg, 6.45 mmol, 3 eq) were reacted at 120 °C. **BPS** (280 mg, 1.11 mmol, 52 %), **tBuDPA-OH** (276 mg, 538 µmol, 25 %) and dimer (129 mg, 268 µmol, 17 %) were obtained.

tBuDPA-OH:

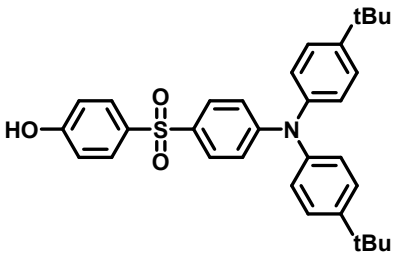

^{1}H NMR (300 MHz, DMSO-d_6) δ 10.57 (s, 1H), 7.71 – 7.67 (m, 2H), 7.65 (d, J = 9.0 Hz, 2H), 7.44 – 7.36 (m, 4H), 7.10 – 7.06 (m, 4H), 6.92 – 6.88 (m, 2H), 6.78 (d, J = 9.0 Hz, 2H), 1.27 (s, 18H).

^{13}C NMR (75 MHz, DMSO-d_6) δ 161.55, 151.49, 147.70, 142.81, 132.09, 131.57, 129.29, 128.56, 126.72, 125.90, 117.54, 115.91, 34.15, 31.06.

HRMS (ESI-TOF): calculated for $C_{28}H_{27}NO_3S$: 458.1789, found: 458.1784.

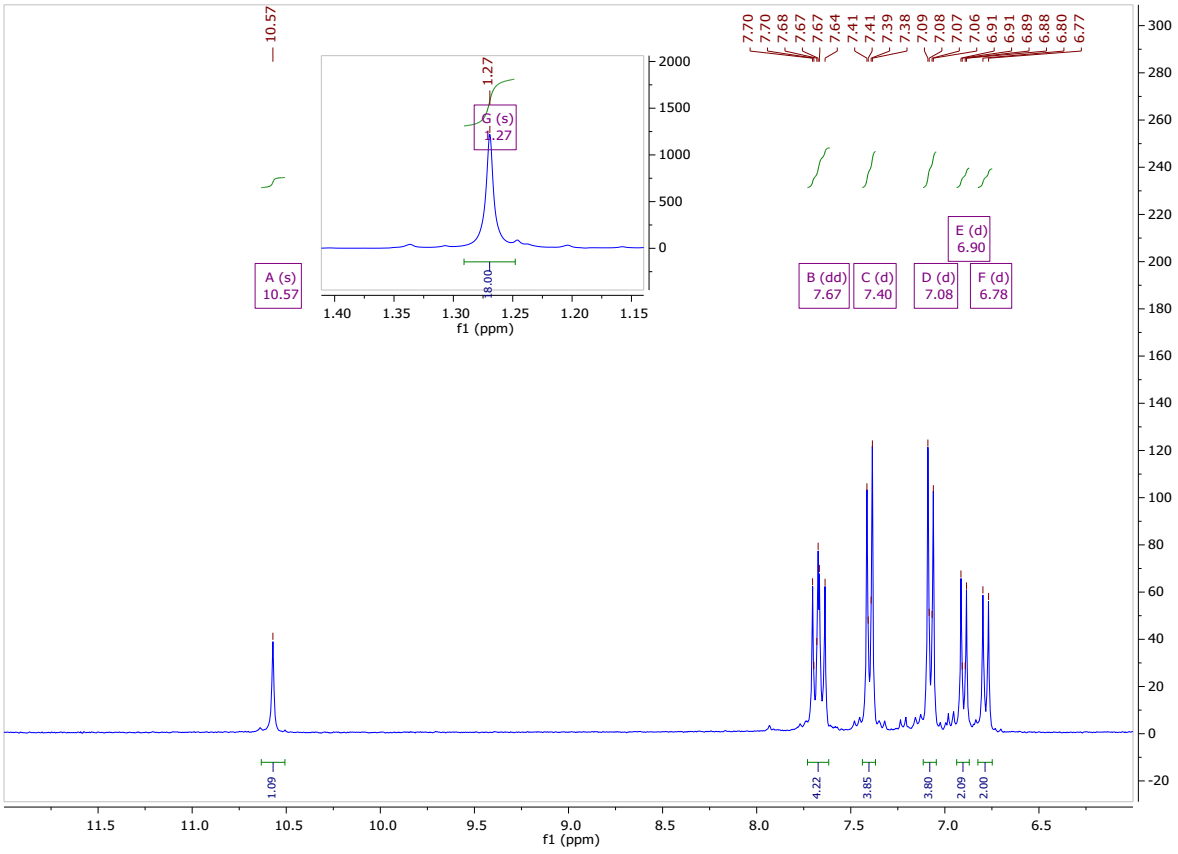

Figure S7: ^{1}H NMR of **tBuDPA-OH** obtained from entry 3 (DMSO-d_6, 300 MHz).

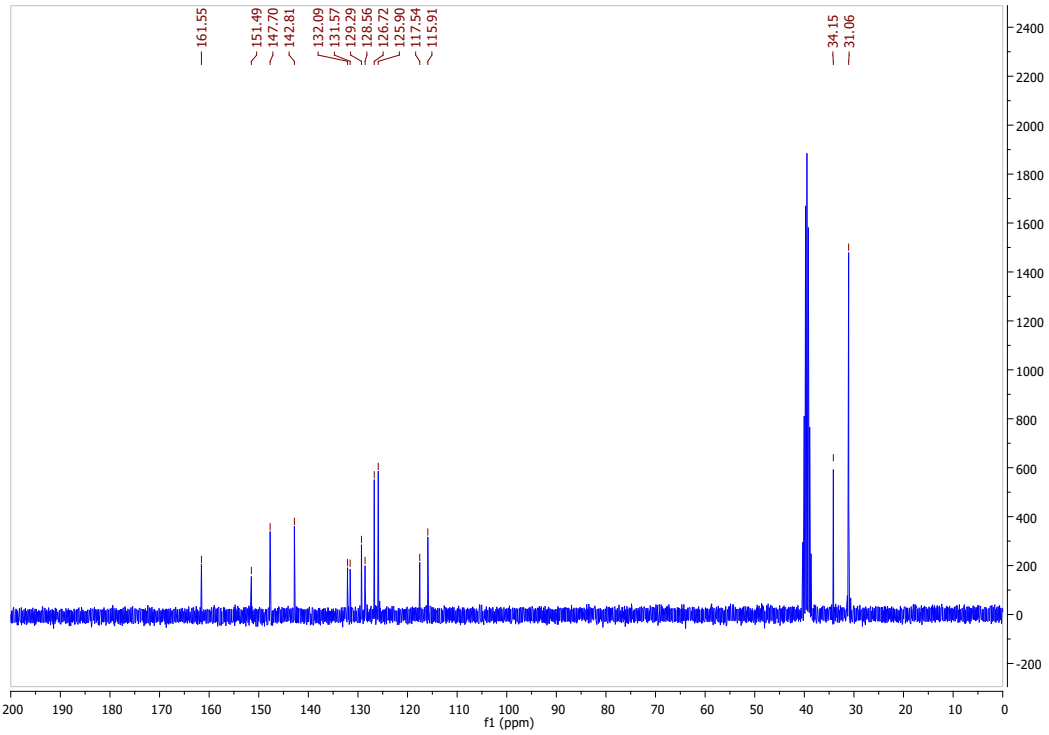

Figure S8 : ^{13}C NMR of **tBuDPA-OH** obtained from entry 3 (DMSO-d_6, 75 MHz).

Dimer:

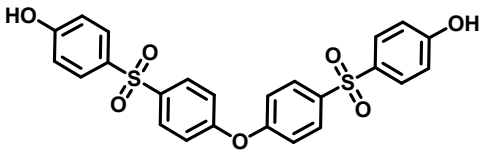

^{1}H NMR (300 MHz, DMSO) δ 10.67 (s, 2H), 7.91 (d, J = 9.0 Hz, 4H), 7.77 (d, J = 8.9 Hz, 4H), 7.24 (d, J = 8.9 Hz, 4H), 6.93 (d, J = 8.9 Hz, 4H).

^{13}C NMR (75 MHz, DMSO-d_6) δ 162.05, 158.98, 137.67, 130.79, 129.81, 129.60, 129.30, 119.68, 116.13, 115.90.
HRMS (ESI-TOF): calculated for $C_{24}H_{18}O_7S_2$: 483.0567, found: 483.0577.

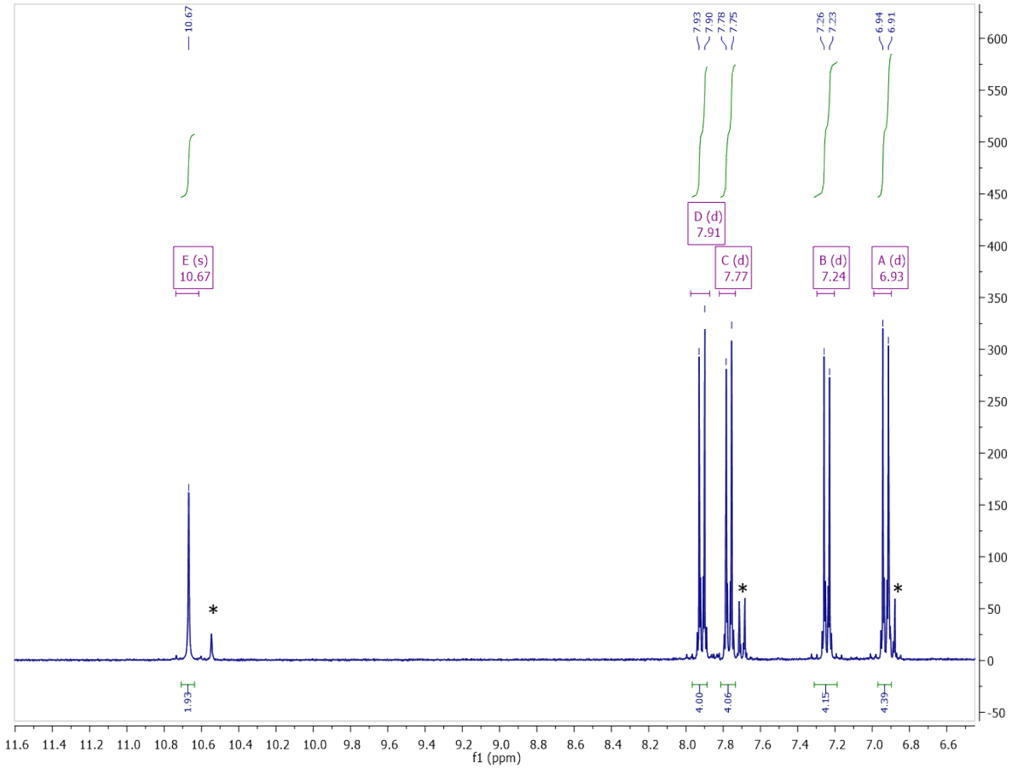

Figure S9 : ^{1}H NMR of dimer obtained from entry 3 (DMSO-d_6, 300 MHz). *Signals of BPS monomer that co-precipitated in the solid product during the precipitation step. This product co-eluate with the dimer during the column chromatography step (see also Figure S3).

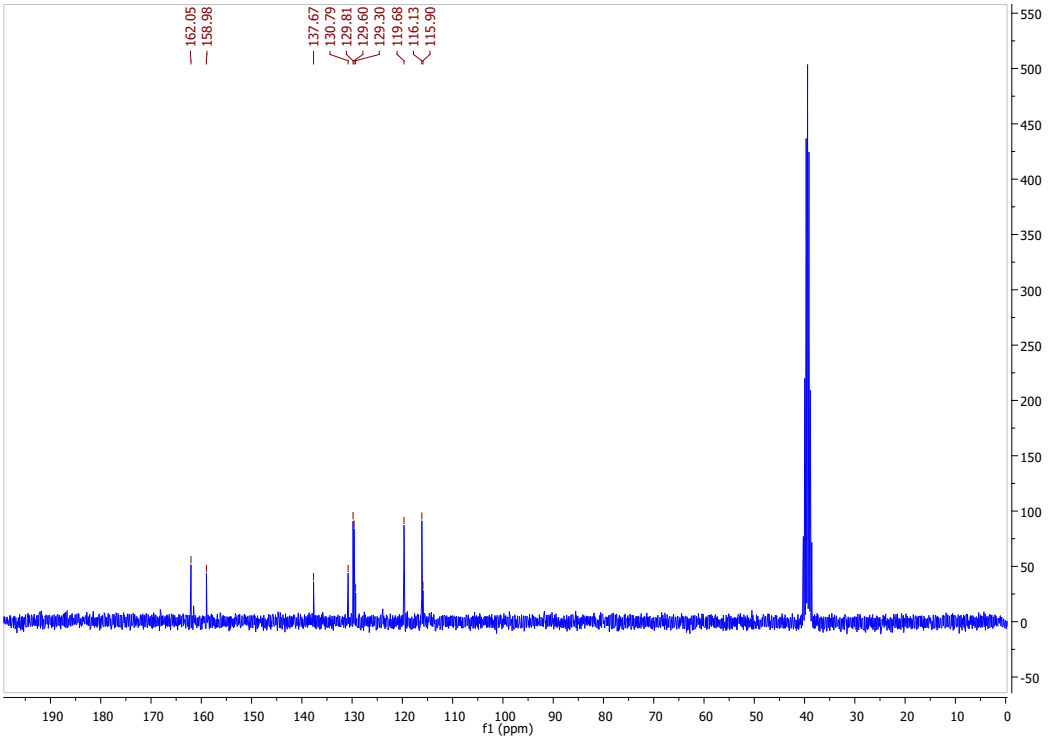

Figure S10 : ^{13}C NMR of the dimer obtained from entry 3 (DMSO-d_6, 75 MHz).

Table 1, Entry 4:

DPA (1.09 g, 6.45 mmol, 3 eq) and NaH (60 % in mineral oil, 257.98 mg, 6.45 mmol, 3 eq) were reacted at 120 °C. **BPS** (183 mg, 0.73 mmol, 34 %), **DiDPA** (244 mg, 452 µmol, 21 %) **DPA-OH** (111 mg, 280 µmol, 13 %) and dimer (164 mg, 340 µmol, 31 %) were obtained.

DiDPA:

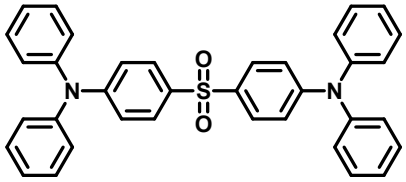

^{1}H NMR (300 MHz, DMSO-d_6) δ 7.70 – 7.66 (m, 4H), 7.44 – 7.36 (m, 8H), 7.25 – 7.13 (m, 12H), 6.89 – 6.83 (m, 4H).

^{13}C NMR (75 MHz, DMSO) δ 151.33, 145.48, 143.35, 132.12, 130.01, 129.11, 128.68, 126.26, 125.37, 119.58, 118.42, 116.64.

HRMS (ESI-TOF): calculated for $C_{36}H_{28}N_2O_2S$: 553.1944, found: 553.1949.

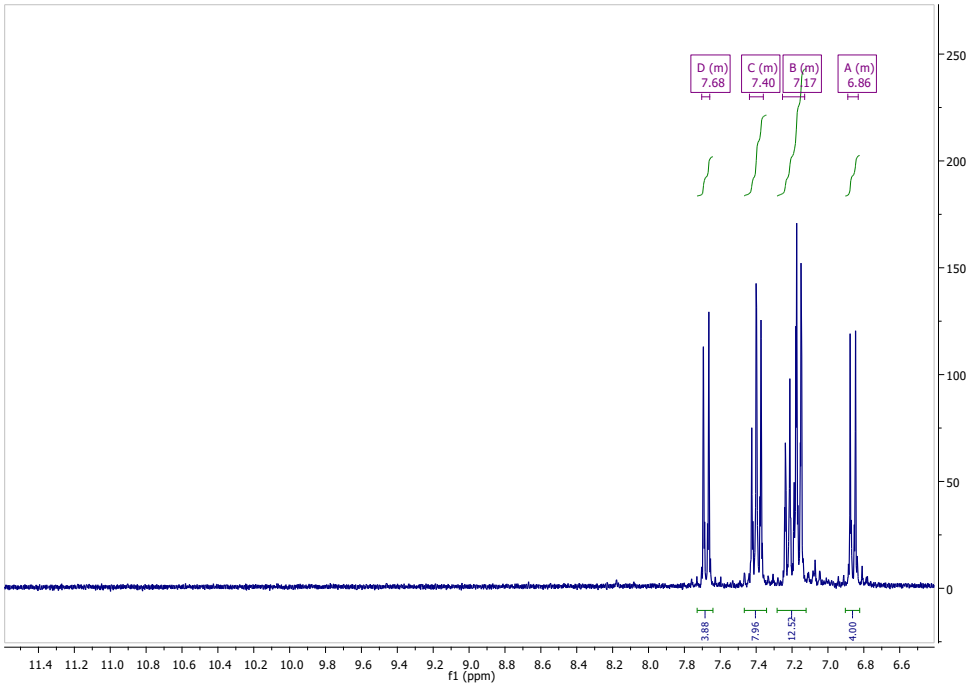

Figure S11 : ^{1}H NMR of **DiDPA** obtained from entry 4 (DMSO-d_6, 300 MHz).

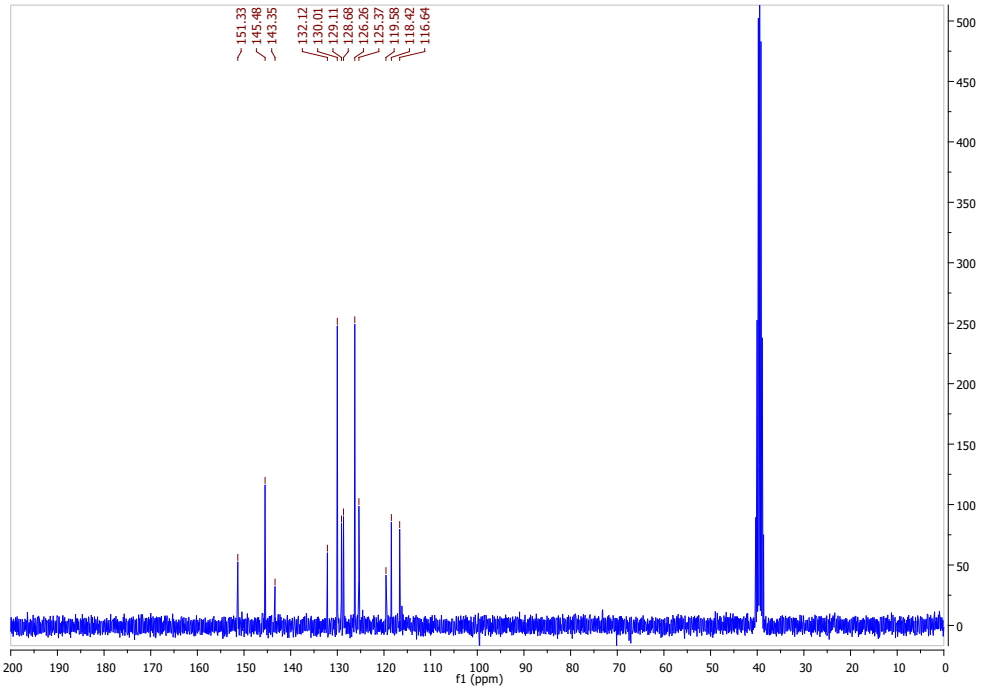

Figure S12 : ^{13}C NMR of **DiDPA** obtained from entry 4 (DMSO-d_6, 75 MHz).

DPA-OH:

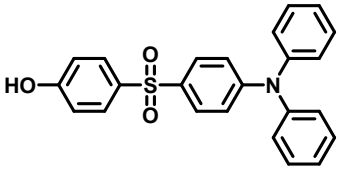

^{1}H NMR (300 MHz, DMSO-d_6) δ 10.60 (s, 1H), 7.73 – 7.66 (m, 4H), 7.43 – 7.35 (m, 4H), 7.24 – 7.13 (m, 6H), 6.93 – 6.88 (m, 2H), 6.88 – 6.82 (m, 2H).

^{13}C NMR (75 MHz, DMSO) δ 161.63, 151.30, 145.52, 132.33, 131.91, 129.99, 129.38, 128.62, 126.23, 125.33, 118.46, 115.96.

HRMS (ESI-TOF): calculated for $C_{24}H_{19}NO_3S$: 402.1158, found: 402.1147.

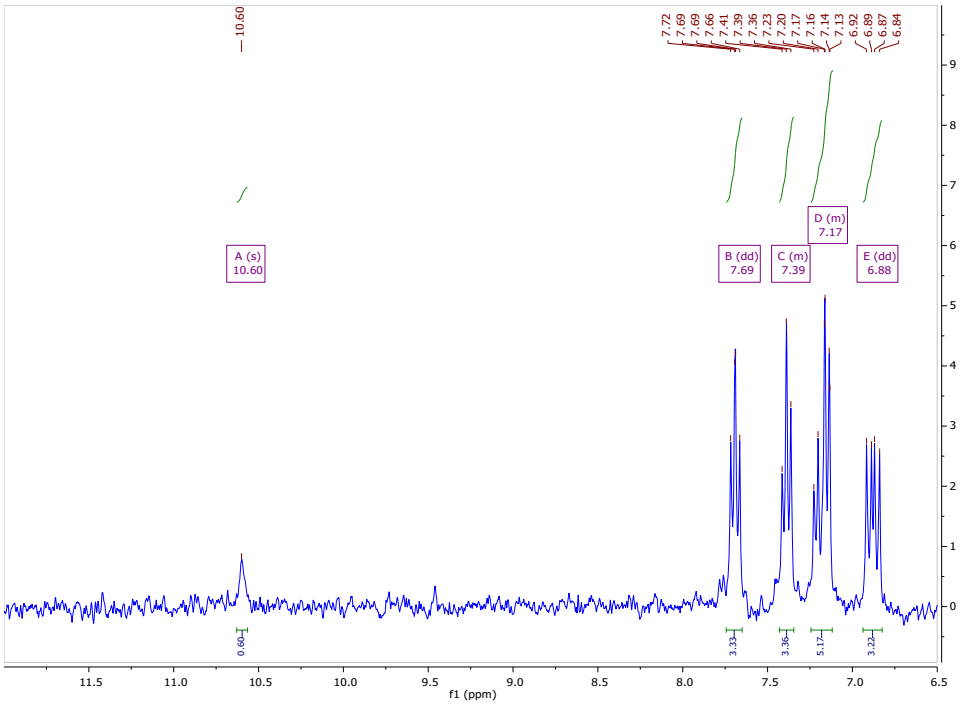

Figure S13 : ^{1}H NMR of **DPA-OH** obtained from entry 4 (DMSO-d_6, 300 MHz).

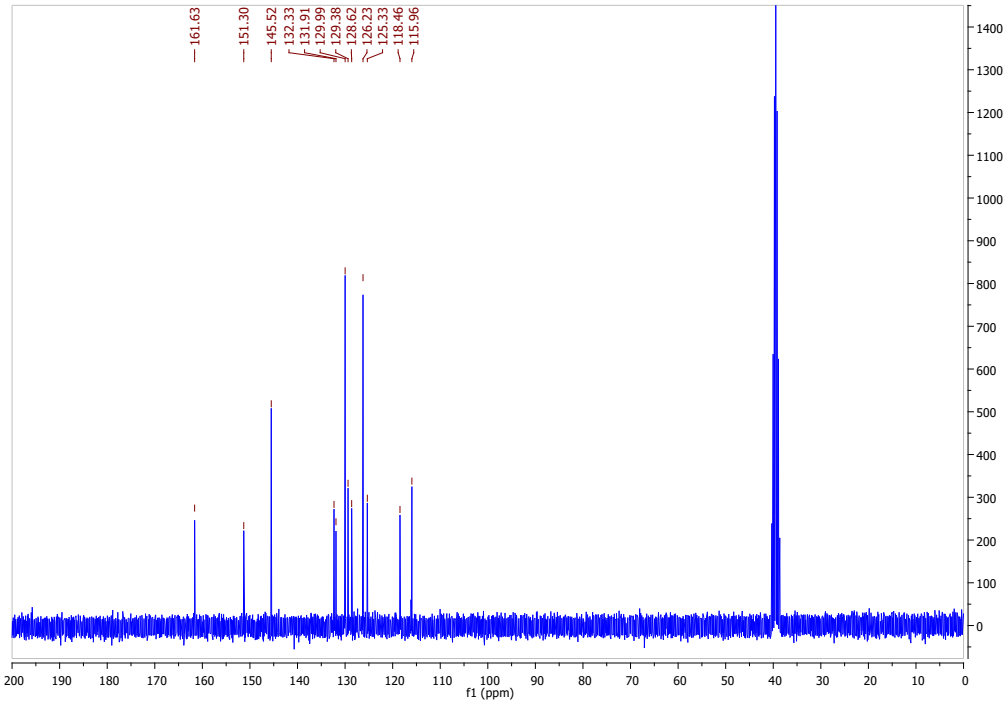

Figure S14 : ^{13}C NMR of **DPA-OH** obtained from entry 4 (DMSO-d_6, 75 MHz).

Table 1, Entry 5:

Carb (1.08 g, 6.45 mmol, 3 eq) and NaH (60 % in mineral oil, 257.98 mg, 6.45 mmol, 3 eq) were reacted at 120 °C. **BPS** (269 mg, 1.07 mmol, 50 %), **DiCarb** (244 mg, 0.44 mmol, 21 %) **Carb-OH** (102 mg, 0.26 mmol, 12 %) and dimer (89 mg, 0.19 mmol, 17 %) were obtained.

DiCarb:

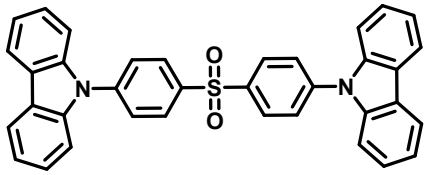

^{1}H NMR (300 MHz, DMSO-d_6) δ 8.36 (d, J = 8.8 Hz, 4H), 8.28 (d, J = 7.2 Hz, 4H), 8.02 (d, J = 8.8 Hz, 4H), 7.57 (d, J = 8.2 Hz, 4H), 7.51 – 7.42 (m, 4H), 7.35 (dd, J = 10.9, 3.9 Hz, 4H).

^{13}C NMR (75 MHz, DMSO) δ 141.74, 139.64, 139.25, 138.81, 129.74, 127.25, 126.52, 125.44, 123.27, 122.31, 120.91, 120.64, 120.10, 118.41, 110.86, 109.87.

HRMS (ESI-TOF): calculated for $C_{36}H_{24}N_2O_2S$: 549.1631, found: 549.1635.

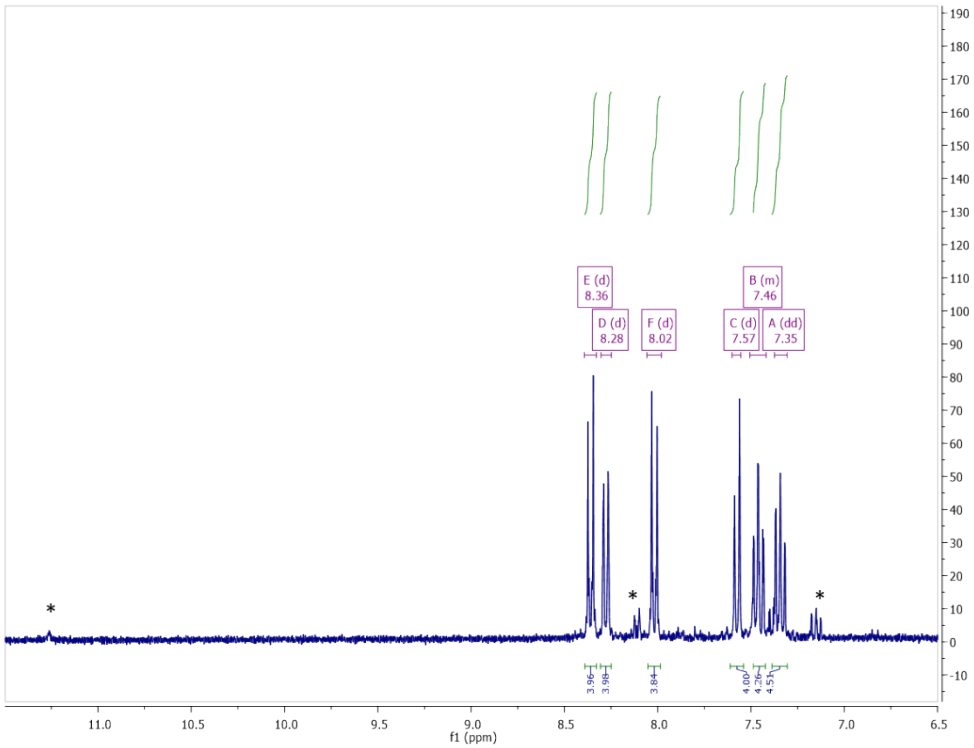

Figure S15 : ^{1}H NMR of **DiCarb** obtained from entry 5 (DMSO-d_6, 300 MHz). * Traces of mono-functionalized molecule **Carb-OH**.

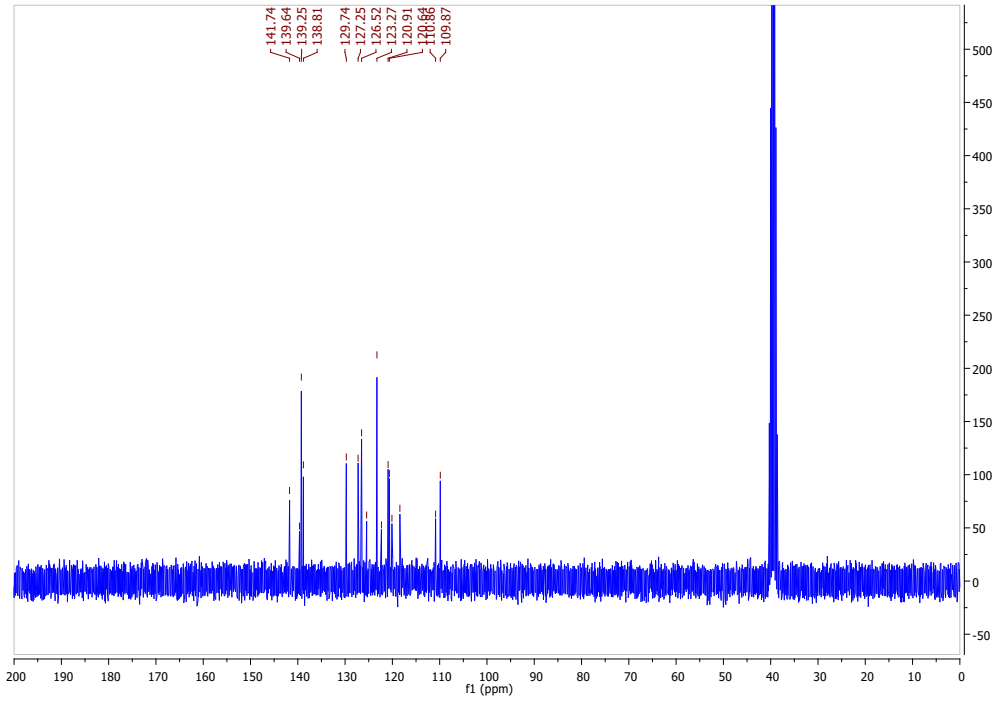

Figure S16 : ^{13}**C** NMR of **DiCarb** obtained from entry 5 (DMSO-d_6, 75 MHz).

Carb-OH:

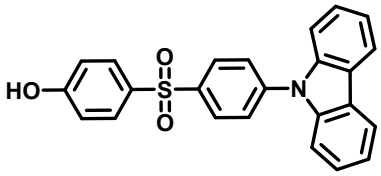

^{1}H NMR (300 MHz, DMSO-d_6) δ 10.77 (s, 1H), 8.26 (d, J = 7.3 Hz, 5H), 8.16 (d, J = 8.8 Hz, 4H), 7.95 – 7.85 (m, 9H), 7.51 (d, J = 7.9 Hz, 4H), 7.44 (dd, J = 7.6, 6.3 Hz, 5H), 7.37 – 7.28 (m, 5H), 6.99 (d, J = 8.9 Hz, 4H).

^{13}C NMR (75 MHz, DMSO) δ 162.38, 140.97, 140.39, 139.32, 130.39, 130.07, 128.97, 127.06, 126.48, 123.17, 120.78, 120.60, 116.29, 109.80.

HRMS (ESI-TOF): calculated for $C_{24}H_{17}NO_3S$: 400.1002, found: 400.1008.

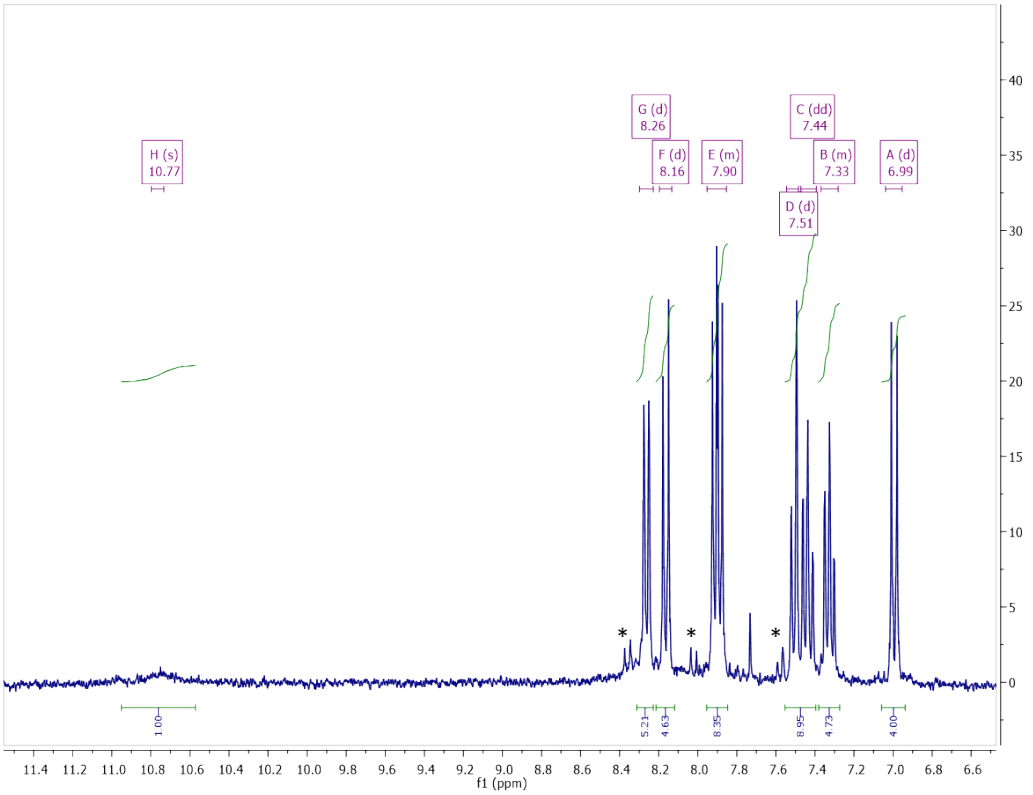

Figure S17 : ^{1}H NMR of **Carb-OH** obtained from entry 5 (DMSO-d_6, 300 MHz). *Traces of di- functionalized molecule **DiCarb**.

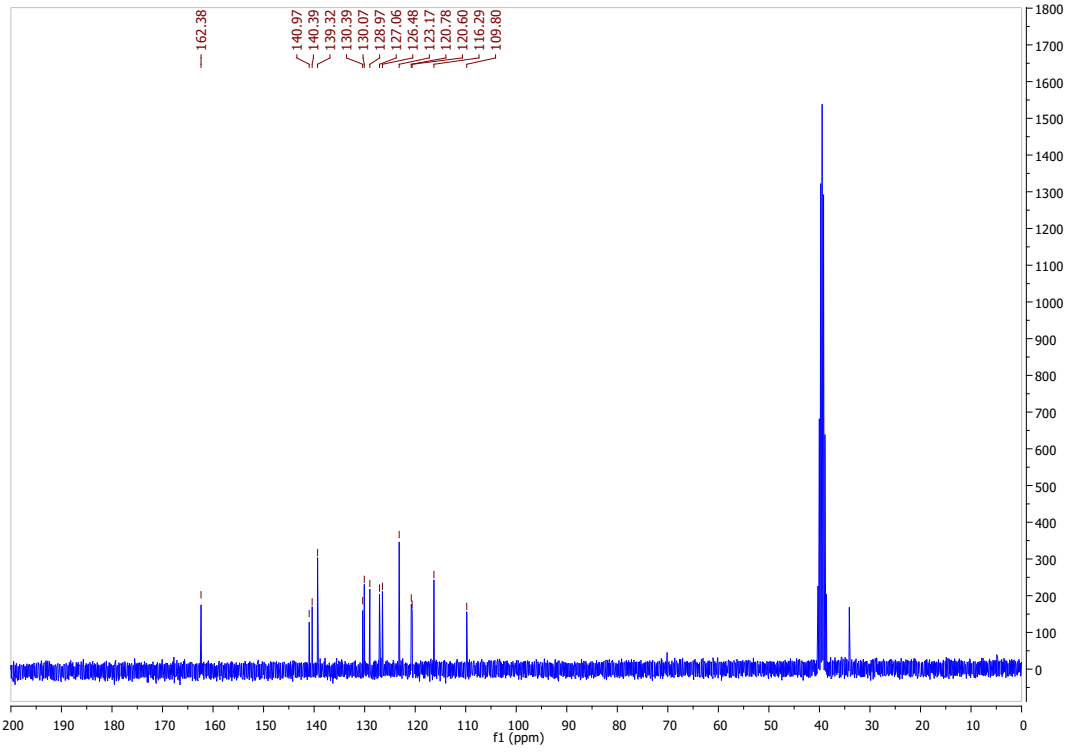

Figure S18: ^{13}C NMR of **Carb-OH** obtained from entry 5 (DMSO-d_6, 75 MHz).

2. Absorption and emission spectra of the luminescent compounds

DiDPA :

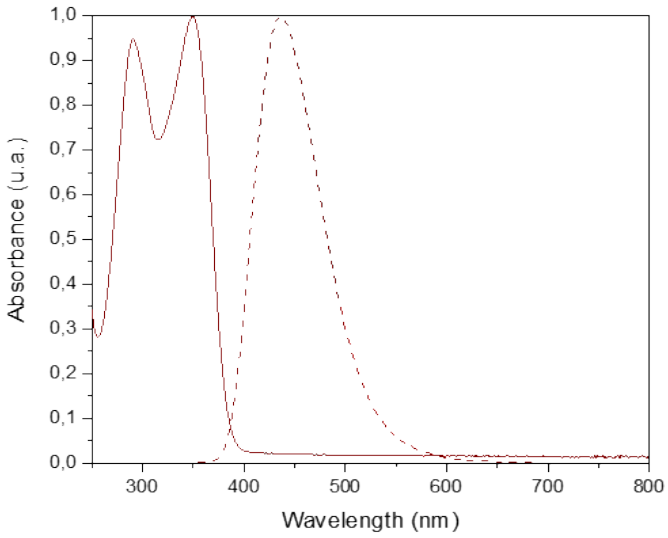

Figure S19 : Absorption (continuous line) and emission (dashed line) spectra of **DiDPA**. (Absorption: 2.10^{-5} M in DCM; Emission: dilution to obtain an optical density of 0.1 in DCM, Excitation at the λ_{max} absorption).

DPA-OH:

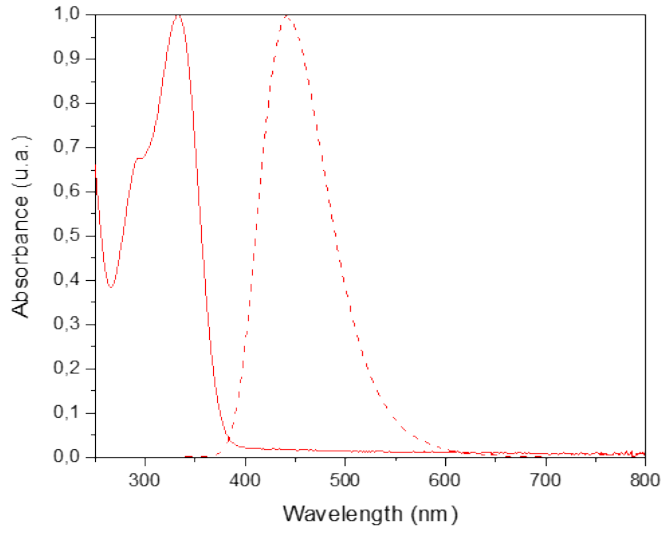

Figure S20 : Absorption (continuous line) and emission (dashed line) spectra of **DPA-OH**. (Absorption: 2.10^{-5} M in DCM; Emission: dilution to obtain an optical density of 0.1 in DCM, Excitation at the λ_{max} absorption).

tBuDPA-OH:

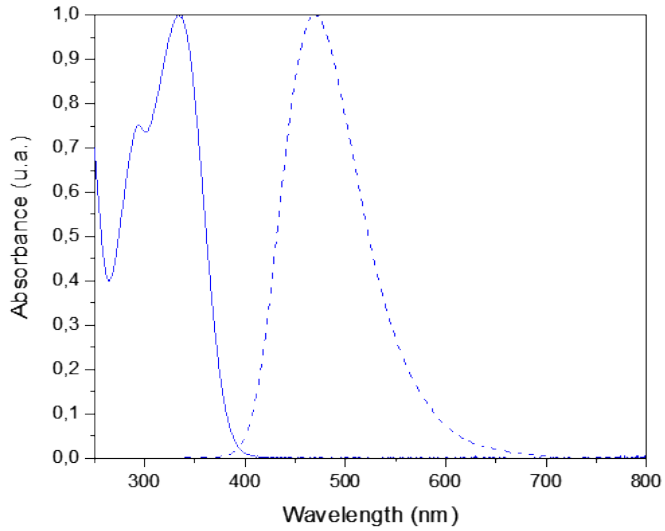

Figure S21: Absorption (continuous line) and emission (dashed line) spectra of **tBuDPA-OH**. (Absorption: 2.10^{-5} M in DCM; Emission: dilution to obtain an optical density of 0.1 in DCM, Excitation at the λ_{max} absorption).

DiCarb:

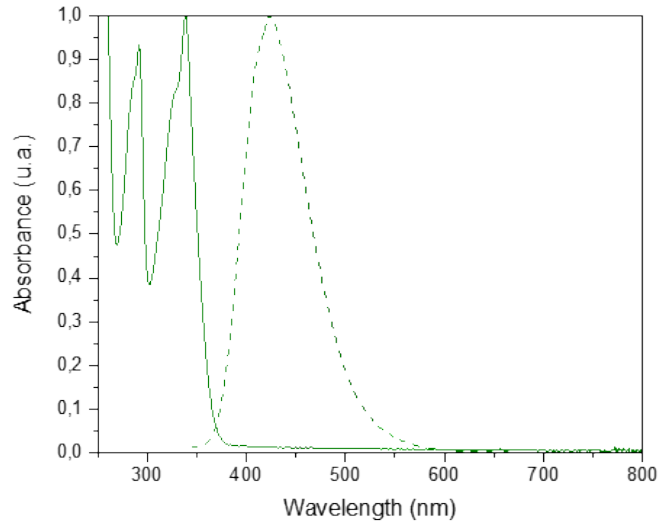

Figure S22: Absorption (continuous line) and emission (dashed line) spectra of **DiCarb**. (Absorption: 2.10^{-5} M in DCM; Emission: dilution to obtain an optical density of 0.1 in DCM, Excitation at the λ_{max} absorption).

Carb-OH:

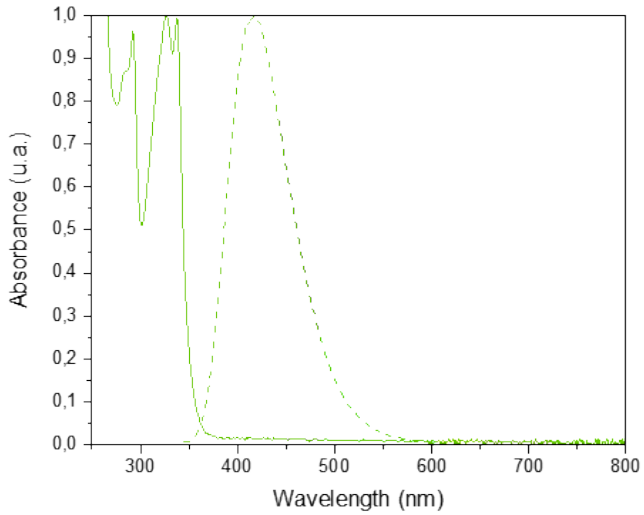

Figure S23: Absorption (continuous line) and emission (dashed line) spectra of **Carb-OH**. (Absorption: 2.10^{-5} M in DCM; Emission: dilution to obtain an optical density of 0.1 in DCM, Excitation at the λ_{max} absorption).

3. DFT modelling of the luminescent materials

Density Functional Theory (DFT) calculations were performed using the NWChem software (version 7.0.0).[1] We chose the B3LYP functional and a 6-31G* basis set for the all-electron calculations. All structures have been geometry optimized without symmetry constraints. The frontier orbitals of the relaxed structures have been visualized with the Jmol software.[2]

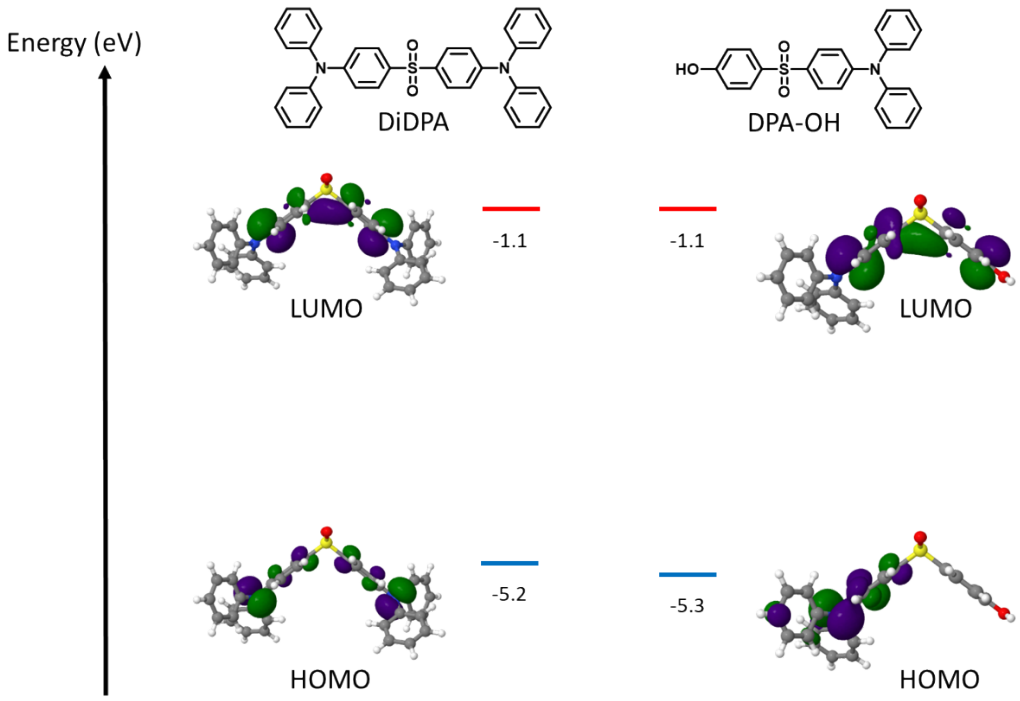

Figure S24: HOMO and LUMO levels modelling of the optimised structures of **DiDPA** and **DPA-OH** (DFT/B3LYP/6-31G*, DFT optimized structure, isovalue 0.02).

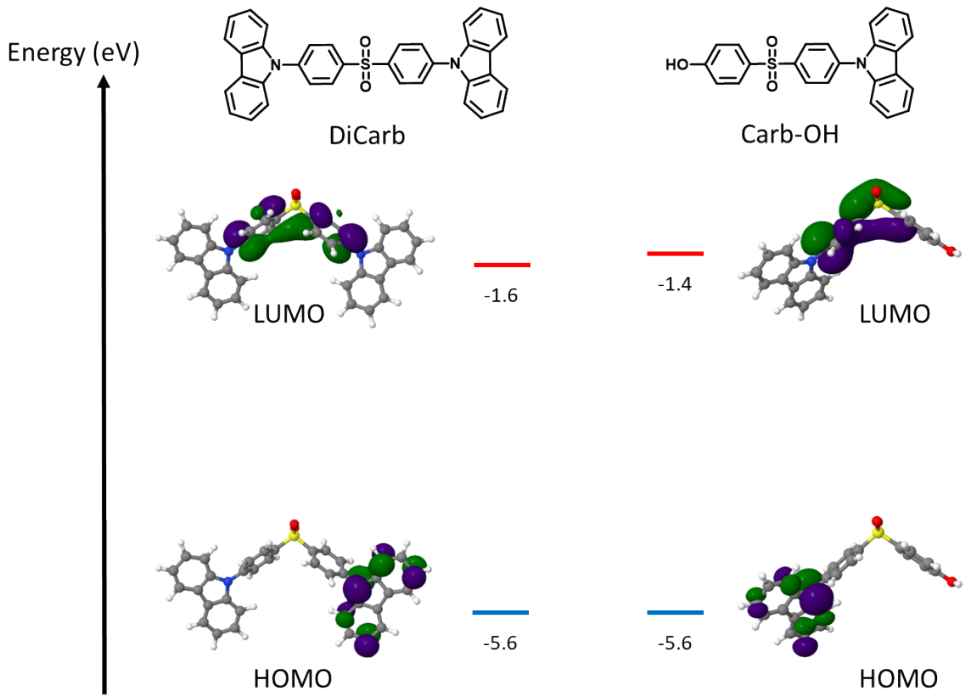

Figure S25: HOMO and LUMO levels modelling of the optimised structures of **DiCarb** and **Carb-OH** (DFT/B3LYP/6-31G*, DFT optimized structure, isovalue 0.02).

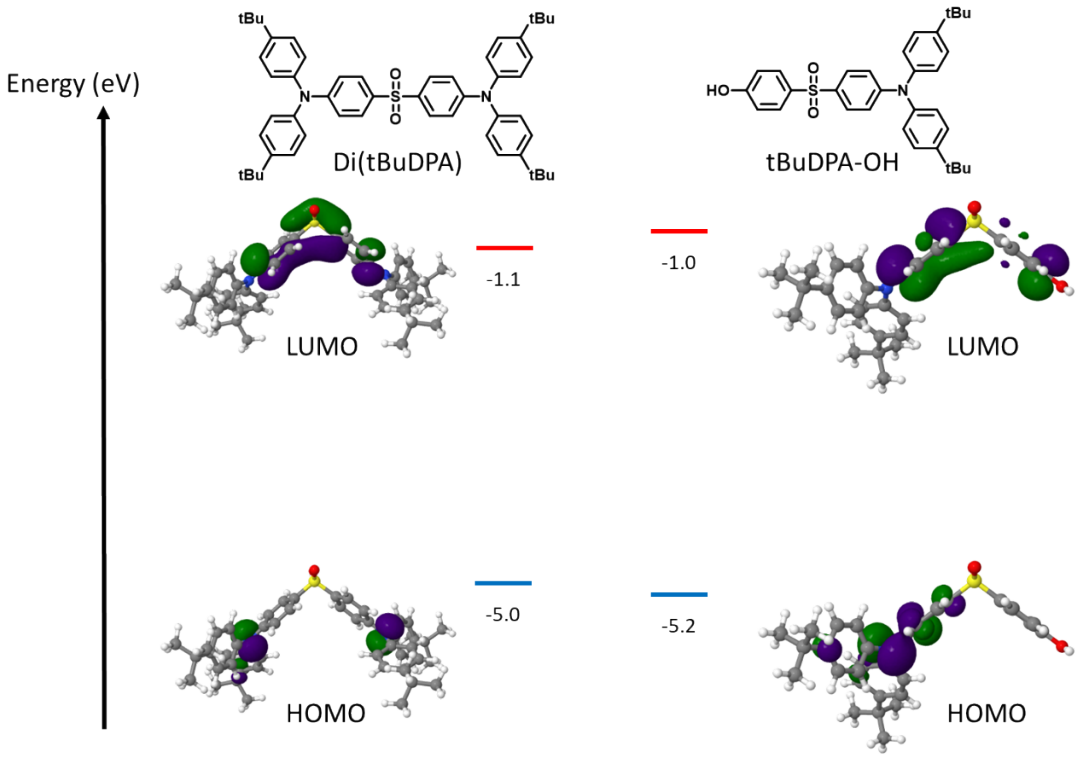

Figure S26: HOMO and LUMO levels modelling of the optimised structures of **Di(tBuDPA)** (not obtained) and **tBuDPA-OH** (DFT/B3LYP/6-31G*, DFT optimized structure, isovalue 0.02).

4. Photoluminescence decay

Time-resolved emission spectra under 380nm excitation have been obtained using a pulsed laser diode PLP-10 from Hamatsu emitting at 375 nm. Emitted light was collected using a monochromator from Andor (Kymera 193i) with a grating of 300 lines/mm. Detection is performed using a hybrid photomultiplier tube (HPM 100-40c) from Becker & Hickl GmbH. Time-resolved analysis is performed using a multichannel counter MCS6A from Fast ComTec (0.8 ns/ channel). A custom software drives the monochromator and records the decay time for each wavelength. The reconstruction of the wavelength resolved decay time measurement is performed offline. The presented decay is reconstructed for emission wavelengths between 430 and 470nm, as indicated with the vertical orange lines in the 2D map. A bi-exponential fitting describes correctly the decay over the first 4 orders of magnitudes (dashed red curve) and lead to a first decay time t_1 of 5.1 ns and a second decay time t_2 of 79.2 ns.

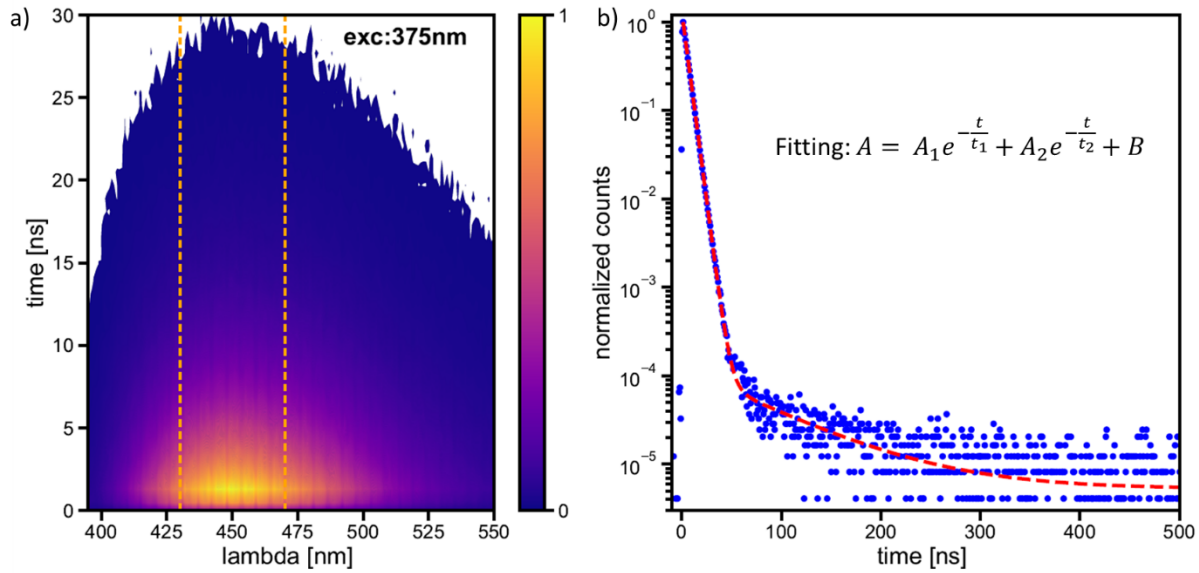

Figure S27: Photoluminescence decay of a DiDPA solution (diluted to obtain an optical density of 0.1 in DCM) of the full spectrum (a) and from the integrated area between 430nm to 470nm (dashed orange lines) (b).

References:

[1] E. Aprà, E. J. Bylaska, W. A. de Jong, N. Govind, K. Kowalski, T. P. Straatsma, M. Valiev, H. J. J. van Dam, Y. Alexeev, J. Anchell, V. Anisimov, F. W. Aquino, R. Atta-Fynn, J. Autschbach, N. P. Bauman, J. C. Becca, D. E. Bernholdt, K. Bhaskaran-Nair, S. Bogatko, P. Borowski, J. Boschen, J. Brabec, A. Bruner, E. Cauët, Y. Chen, G. N. Chuev, C. J. Cramer, J. Daily, M. J. O. Deegan, T. H. Dunning, M. Dupuis, K. G. Dyall, G. I. Fann, S. A. Fischer, A. Fonari, H. Früchtl, L. Gagliardi, J. Garza, N. Gawande, S. Ghosh, K. Glaesemann, A. W. Götz, J. Hammond, V. Helms, E. D. Hermes, K. Hirao, S. Hirata, M. Jacquelin, L. Jensen, B. G. Johnson, H. Jónsson, R. A. Kendall, M. Klemm, R. Kobayashi, V. Konkov, S. Krishnamoorthy, M. Krishnan, Z. Lin, R. D. Lins, R. J. Littlefield, A. J. Logsdail, K. Lopata, W. Ma, A. V Marenich, J. Martin del Campo, D. Mejia-Rodriguez, J. E. Moore, J. M. Mullin, T. Nakajima, D. R. Nascimento, J. A. Nichols, P. J. Nichols, J. Nieplocha, A. Otero-de-la-Roza, B. Palmer, A. Panyala, T. Pirojsirikul, B. Peng, R. Peverati, J. Pittner, L. Pollack, R. M. Richard, P. Sadayappan, G. C. Schatz, W. A. Shelton, D. W. Silverstein, D. M. A. Smith, T. A. Soares, D. Song, M. Swart, H. L. Taylor, G. S. Thomas, V. Tipparaju, D. G. Truhlar, K. Tsemekhman, T. Van Voorhis, Á. Vázquez-Mayagoitia, P. Verma, O. Villa, A. Vishnu, K. D. Vogiatzis, D. Wang, J. H. Weare, M. J. Williamson, T. L. Windus, K. Woliński, A. T. Wong, Q. Wu, C. Yang, Q. Yu, M. Zacharias, Z. Zhang, Y. Zhao, R. J. Harrison, *J. Chem. Phys.* **2020**, *152*, 184102.

[2] Jmol development team, 2016. *Jmol*, Available at: http://jmol.sourceforge.net/.